

# COUPLING IMPEDANCE OF THE COLLIMATOR WITHOUT RF-SHIELDS AT THE RCS IN J-PARC

Y. Shobuda\*, K. Okabe, J. Kamiya, and K. Moriya  
J-PARC Center, JAEA/KEK, [319-1192] Ibaraki, JAPAN

## Abstract

All holes on the chamber walls of synchrotrons should be filled with the radiofrequency (RF)-shields to suppress coupling impedances that excite beam instabilities. In a synchrotron, titanium nitride (TiN)-coated RF-shields are installed with collimators. If the holes, through which the collimator jaw enters and exits the chamber, are filled with such RF-shields, the shields may break down as the dynamic coefficient of TiN increases in vacuum. At the Rapid Cycling Synchrotron (RCS), the RF-shields are eliminated from the collimator after demonstrating that the effect due to the RF-shields is negligible on the impedance at low frequencies.

## INTRODUCTION

At the RCS in J-PARC [1], the aim is to realize a megawatt-class beam. A 1-MW beam can be realized at the RCS by accelerating two bunched beams, each containing  $4.15 \times 10^{13}$  particles per bunch, from 400-MeV to 3-GeV at a repetition rate of 25 Hz.

To suppress the radioactive residual dose level along the ring, six collimators are installed in the RCS, and they confine the beam loss area into a specified region. The collimator jaws (blocks) should be adjustable to optimize the beam loss. Hence, the holes through which the jaws intrude into the chamber are unavoidable in the collimator. Meanwhile, suppressing coupling impedances [2] along the ring is crucial to realize the high-intensity beams [3,4]. Therefore, all holes are plugged in by the RF-shields at the RCS.

The surfaces of collimator blocks and RF-shields are typically coated with TiN to suppress the electron clouds (which are generated by the collision of beam halo with the blocks) that cause electron cloud instabilities [5, 6].

Recently, we fabricated a new collimator to replace the old one that had malfunctioned. Before installation, the performance of the new collimator was thoroughly tested in vacuum; during the test, the blocks were intruded into and taken out of the chamber. Finally, the RF-shields filling the holes broke down.

We discovered that this problem is caused by the enhancement of the dynamic friction coefficient of TiN “in vacuum” [7]. This finding implies that the breakdown of TiN-coated RF-shields used to fill holes could affect all collimators. The simplest solution to eliminate this problem is to install collimators without RF-shields.

In this paper, we discuss whether this scheme is acceptable for a low-energy machine such as the RCS. First, we studied the beam impedances of the collimator with RF-

shields, and then examined the increase in impedances after removing the RF-shields.

## ESTIMATION OF IMPEDANCE BY SIMPLE MODELS

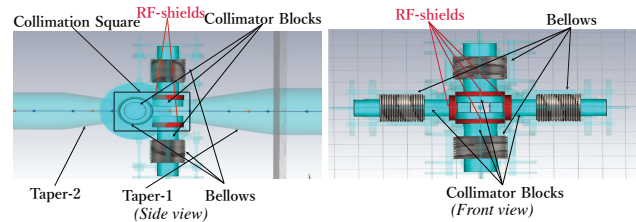


Figure 1: Schematics of the collimators at the RCS.

Figure 1 shows the schematics of the collimator at the RCS [7]. It consists of a collimation square sandwiched by taper-1 and taper-2. Here the radii of taper-1 and taper-2 change from end-to-end. The collimation square has a uniform cylindrical chamber with two horizontal and vertical holes in the beam direction at the different longitudinal locations. Four cylindrical collimator blocks with radii 100 mm are intruded into the collimation square through the holes. Each collimator block is connected to the bellows surrounding the upper half of the block. The collimator blocks can be put in and taken out of the collimation square by compressing or stretching the bellows. Thus, the collimator block and the bellows form a large coaxial structure in the collimator. In order to prevent the electromagnetic (EM) fields from being stored in the structure, the holes are typically plugged in by TiN-coated RF-shields.

The analytical formula for the longitudinal impedance  $Z_L$  is known for a cylindrical chamber with radius  $a$  instantly changing to  $a - h$  at a location and returning to  $a$  after longitudinal length  $g$  [8] :

$$Z_L(\omega) = j \frac{\omega Z_0 h^2}{2\pi^2 c a} \left( 2 \log \frac{2\pi a}{h} + 1 \right), \quad (1)$$

where  $j$  is the imaginary unit;  $Z_0 = 120\pi$  [ $\Omega$ ];  $\omega = 2\pi f$  is the angular frequency;  $f$  [Hz] is the frequency; and  $c$  [m/s] is velocity of light. We use this formula to estimate the impedance of the collimator with RF-shields. Now, the transverse impedance  $Z_T$  is approximated as [9]

$$Z_T(\omega) \approx \frac{2c Z_L(\omega)}{\omega a^2} = j \frac{Z_0 h^2}{\pi^2 a^3} \left( 2 \log \frac{2\pi a}{h} + 1 \right), \quad (2)$$

referring to the Panofsky-Wenzel theorem [10].

For  $h = 55$  mm and  $a = 95$  mm,

$$Z_L(\omega) = j0.0734768 f [\text{MHz}], \quad [\Omega], \quad (3)$$

$$Z_T(\omega) = j0.777454, \quad [\text{k}\Omega/\text{m}], \quad (4)$$

which do not excite instabilities in the RCS under 1-MW operation.

Content from this work may be used under the terms of the CC BY 3.0 licence (© 2019). Any distribution of this work must maintain attribution to the author(s), title of the work, publisher, and DOI

At the RCS, the 515 mm-long cylindrical chamber embedded in the collimation square is sandwiched by taper-1 whose radius changes from 95 mm to 189.5 mm over a length of 526.5 mm, and taper-2 whose radius changes from 95 mm to 148.5 mm over a length of 291.5 mm. In order to consider the effect of the tapers, a more precise estimation was performed numerically with two-dimensional simulation (2D) code ABCI [11] by assuming an axisymmetric structure, where all the materials are assumed to be perfectly conductive.

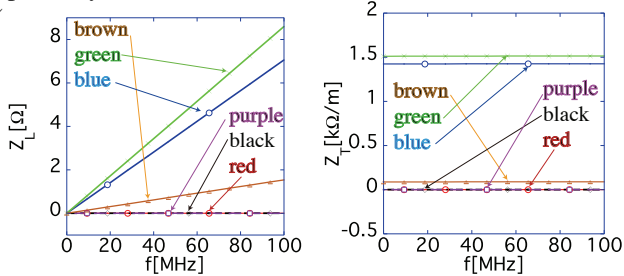


Figure 2: Simulations of  $Z_L$  (left) and  $Z_T$  (right) by ABCI.

The simulation results are shown in Figure 2. The figures on the left and right show  $Z_L$  and  $Z_T$ , respectively. The purple-□- and brown-△- lines show the real and imaginary parts of the impedances, respectively, with  $h = 0$ . The result represents the real collimator with RF-shields, where the edges of four collimator blocks are set on the inner surface of the cylindrical chamber in the collimation square; hereafter, this chamber will be referred to as “a reference chamber (condition)”. The black-◇- and green-×- lines show the real and imaginary parts of the impedances, respectively, with  $h = 55$  mm and  $g = 200$  mm, including the taper effects. The red-o- and blue-o- lines show the real and imaginary parts of the impedance, respectively, excluding the taper effects. A comparison of the red-o- and blue-o- lines with the results obtained using Eqs.(3) and (4) showed us that  $Z_L$  is well estimated by the original analytical formula (1), while  $Z_T$  is in agreement with the formula (2) within a factor of two. The negligence of the real parts of the impedances in the analytical formulae are validated by the simulation results below 100 MHz.

### ESTIMATION OF IMPEDANCE BY 3D SIMULATIONS AND MEASUREMENTS

In a real collimator, wherein the collimator blocks intrude into the chamber by an amount ( $h > 0$ ), the axisymmetry is broken. Hence, three-dimensional (3D) simulation is necessary to identify the effect of asymmetry and absence of RF-shields on beam impedance.

The 3D simulation code CST [12] can deal with the wake fields of collimators made of stainless steel (with conductivity  $\sigma_c = 1.35 \times 10^6$  S/m). Figure 3 shows  $Z_L$  (left) and  $Z_T$  (right) with  $h = 55$  mm. The black-●-/brown-△- and red-o-/blue-o- lines represent the impedances without and with the RF-shields, respectively, after subtracting the impedance of the reference chamber ( $h = 0$ , with RF-shields). The red-o-/black-●- and blue-o-/brown-△- lines

show the real and imaginary parts of the impedances, respectively.

We find that the 2D simulation tool, as well as analytical formulas (1) and (2), can still be used to estimate the impedances because the realistic 3D simulation results with RF-shields (red-o-/blue-o- in Fig.3) and the 2D simulation results (red-o-/blue-o- in Fig.2) based on the simple model are in good agreement both for  $Z_L$  and  $Z_T$ . The resonance structure is identified at high frequencies in the results without RF-shields, indicating that the wake fields penetrate into the space created between the collimator blocks and the bellows. Hence, we have re-concluded that the RF-shields are beneficial especially for accelerating high-energy, high-intensity short bunched beams.

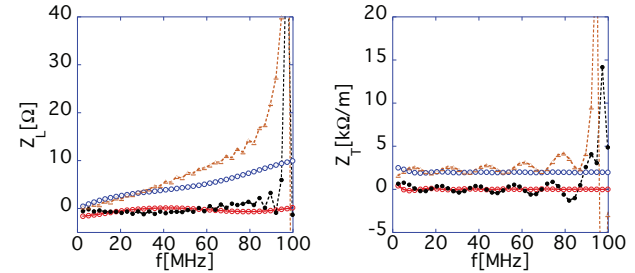


Figure 3: Simulations of  $Z_L$  (left) and  $Z_T$  (right) by CST.

On the other hand, for a low-energy proton machine such as the RCS, owing to the longer bunched beam, the impedance is more important at frequencies below 10 MHz. Figure 3 demonstrates that the resonance structure does not contribute to the enhancement of impedance below 30 MHz both for  $Z_L$  and  $Z_T$ . This is because the fields with wavelengths larger than the hole size cannot recognize the structure inside the space created between the collimator blocks and the bellows. Consequently, we expect that the difference between the impedances without and with the RF-shields should be negligible in the case of the RCS.

Now, let us measure  $Z_L$  and  $Z_T$  by stretching thin (160  $\mu$ m diameter) single- and twin-wires inside the collimator and the reference chamber and observing the respective scattering matrices with a Network Analyzer (NA) [13]. In the measurement, both the ends of the tapers are terminated through the resistors by 50  $\Omega$  N-type connectors for the NA. For the single-wire measurement, the resistors are chosen to match the characteristic impedances  $Z_{cc1}$  and  $Z_{cc2}$  at the very ends of the taper-1 and taper-2, respectively. For the twin-wire measurement, the impedance-bridge must match the characteristic impedances not only for the differential modes ( $Z_{dd1}$  and  $Z_{dd2}$ ) but also for the common ones of the taper-1 and taper-2. All scattering matrices were measured and averaged 3000 times within the temperature fluctuation  $\Delta T \leq 1$  K of the environment to suppress systematic errors. All the single- and twin-wire measurements under different conditions for blocks and RF-shields were performed after fixing the corresponding terminal conditions for the wires, to minimize other systematic errors as small as possible.

The measured scattering matrices are converted to  $Z_L$  and  $Z_T$  by modifying the standard-log formulas [14] as fol-

lows:

$$Z_L(\omega) = -(Z_{cc1} + Z_{cc2}) \log \left[ \frac{S_{cc21}^{(col)}}{S_{cc21}^{(ref)}} \right], \quad (5)$$

$$Z_L(\omega) = -\frac{c(Z_{dd1} + Z_{dd2})}{\omega\Delta^2} \log \left[ \frac{S_{dd21}^{(col)}}{S_{dd21}^{(ref)}} \right], \quad (6)$$

where  $S_{cc(dd)21}^{(col)}$  and  $S_{cc(dd)21}^{(ref)}$  are the transmission coefficients for the collimator and the reference chamber, respectively; the subscripts *cc* and *dd* denote the common and the differential modes, respectively; and  $\Delta$  is the separation between the twin-wires [15].

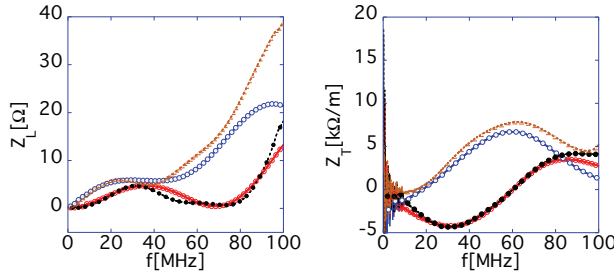


Figure 4: Measurements of  $Z_L(\omega)$  (left) and  $Z_T(\omega)$  (right).

Figure 4 shows the measured  $Z_L$  (left) and  $Z_T$  (right), where the black-●-/brown-△- and red-o-/blue-o- lines represent the impedances without and with the RF-shields, respectively. We see a slight impedance enhancement at low frequencies because of the detachment of RF-shields from the collimator. As expected, we can identify the tendency that the impedance-suppressing effect of the RF-shields becomes more significant toward high frequencies, though the resonance structure cannot be clearly seen in these  $Z_T$  measurements. This may attribute to an incompleteness of matching conditions at both ends of tapers for twin-wires.

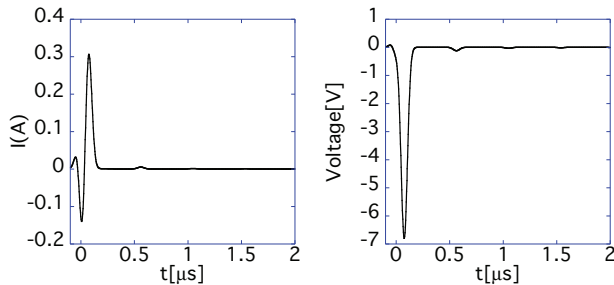


Figure 5: Wall current on the bellows (left) and voltage between the bellows and collimator block (right).

Finally, let us closely investigate the phenomenon inside the bellows to address another concern about removing the RF-shields that the EM fields excited by the high-intensity beam may adversely affect collimator functions by causing heating of the bellows or creating a discharge inside the bellows [16].

Here, let us look into the beam-induced (wall) current on the bellows and the beam-induced voltage between the bellows and the collimator block. The Fourier components for the current and the voltage were simulated with CST [12] by passing a beam with a much smaller longitudinal rms

size  $\sigma_s = 40$  mm through the collimator, and setting the parameter WAKELENGTH=100 m so that the EM fields are sufficiently damped. The current and the voltage for the Gaussian beam with a total charge  $q = 6.64 \mu\text{C}$  and a longitudinal rms size  $\sigma_s = 9$  m, simulating the beam at the RCS, were calculated.

The results are shown in Fig.5. The left and the right figures show the current and the voltage, respectively. Current and voltage excitation occur only for about  $0.3 \mu\text{s}$  and decay rapidly. Since the revolution frequency of the RCS (with two bunches) is 0.86 MHz even at 3-GeV beam energy, the successive beam passage does not cause a buildup of the current and voltage during the acceleration period.

The power consumption on the bellows was explicitly calculated as follows. First, the resistance of the stainless steel bellows with conductivity  $\sigma_c$  and length  $L (= 183.5 \text{ mm})$  was estimated by splitting the bellows into halves along the plane perpendicular to the beam direction to obtain two semi-cylindrical bellows. We assumed the total resistance can be calculated by combining the resistance of two semi-cylindrical bellows in series. Since the inner radius of the bellows with thickness  $\Delta_1 (= 0.3 \text{ mm})$  is approximated by

$$f(x) = \frac{(a_{\text{out}} - \Delta_1 + a_{\text{in}}) - (a_{\text{out}} - \Delta_1 - a_{\text{in}}) \cos \left[ \frac{2\pi x}{\left(\frac{L}{\text{per}}\right)} \right]}{2}, \quad (7)$$

at the RCS, where  $a_{\text{out}} (= 112.5 \text{ mm})$  and  $a_{\text{in}} (= 102.5 \text{ mm})$  are the maximum and minimum radii of the bellows, respectively; and  $L/\text{per} (= 14 \text{ mm})$  is the period of undulation of the radius, the resistance of the bellows  $R(\omega)$  for the wall-current is calculated as

$$R(\omega) = \frac{N_{\text{col}}}{\sigma_c} \int_0^L \frac{dx \sqrt{1 + \left(\frac{df(x)}{dx}\right)^2}}{2\pi f(x)\delta(\omega)}, \quad (8)$$

where  $\delta(\omega)$  is skin depth;  $N_{\text{col}} (= 4)$  is the number of bellows per a collimator. The numerator and denominator in the integrand in Eq.(8) denote the effective path-length and cross section of the wall-current, respectively. Finally, the power consumption at the bellows per a collimator is estimated as  $14 \mu\text{W}$  with a repetition rate of 25 Hz by evaluating  $\delta(\omega)$  at  $f = 10 \text{ MHz}$ . The power consumption is negligible under routine beam operation conditions at the RCS.

## SUMMARY

No significant obstacles were observed at the RCS in the 1-MW-equivalent operation [17], after detaching the RF-shields from the collimator both from the viewpoint of impedance exciting beam-instabilities and from the mechanical viewpoint regarding the collimator functions.

Through simulation and measurement, we demonstrated that the effect of the RF-shields on collimator impedance is negligible at low frequencies. To overcome the problem that the TiN-coated RF-shields may break down in vacuum, the RF-shields may be removed from the collimator. Instead, the inner surface of the bellows must be perfectly coated with TiN to suppress electron cloud instabilities.

## REFERENCES

- [1] J-PARC, <http://j-parc.jp/index-e.html>
- [2] A. W. Chao, *Physics of Collective Beam Instabilities in High Energy Accelerators*, New York, USA: Wiley, 1993.
- [3] Y. Shobuda *et al.*, “Theoretical elucidation of space charge effects on the coupled-bunch instability at the 3 GeV rapid cycling synchrotron at the Japan Proton Accelerator Research Complex”, *Prog. Theor. Exp. Phys.*, vol. 2017, 1, 013G01, Jan. 2017; <https://doi.org/10.1093/ptep/ptw169>
- [4] P. K. Saha *et al.*, “Simulation, measurement, and mitigation of beam instability caused by the kicker impedance in the 3-GeV rapid cycling synchrotron at the Japan Proton Accelerator Research Complex”, *Phys. Rev. Accel. Beams*, vol. 21, 024203, Feb. 2018; <https://doi.org/10.1103/PhysRevAccelBeams.21.024203>
- [5] K. Ohmi, T. Toyama, and C. Ohmori, “Electron cloud instability in high-intensity proton rings”, *Phys. Rev. ST Accel. Beams*, vol. 5, 114402, Nov. 2002; <https://journals.aps.org/prab/abstract/10.1103/PhysRevSTAB.5.114402>
- [6] K. Ohmi, T. Toyama, and C. Ohmori, “Erratum”, *Phys. Rev. ST Accel. Beams*, vol. 6, 029901, Feb. 2003; <https://doi.org/10.1103/PhysRevSTAB.6.029901>
- [7] K. Okabe *et al.*, “An improvement of the beam collimator in the J-PARC 3 GeV rapid cycling synchrotron”, to be submitted to *Nucl. Instru. Meth.*.
- [8] S. S. Kurennoy and G. V. Stupakov, “A new method for calculation of low-frequency coupling impedance”, *Particle Accelerators*, vol. 45, 95, Mar. 1994; <https://cds.cern.ch/record/250977/files/p95.pdf>
- [9] Y. H. Chin, S. Lee, Y. Shobuda, K. Takata, T. Toyama, and H. Tsutsui, “Impedance and radiation generated by a ceramic chamber with RF shields and TiN coating”, in *Proc. 39th ICFA Advanced Beam Dynamics Workshop on High-Intensity and High-Brightness Hadron Beams (HB’06)*, Tsukuba, Japan, May-Jun. 2006, paper TUBX01, pp. 125–127.
- [10] W. Panofsky and W. Wenzel, “Some considerations concerning the transverse deflection of charged particles in radio-frequency fields”, *Rev. Sci. Instr.*, vo. 27, 967, Nov. 1956; <https://aip.scitation.org/doi/10.1063/1.1715427>
- [11] Y. H. Chin, “User’s guide for ABCI”, KEK Report No. 2005-06, 2005; <http://abci.kek.jp/abci.htm>
- [12] CST STUDIO SUITE, <https://www.cst.com>
- [13] Keysight, <https://www.keysight.com/us/en/home.html>
- [14] W. Chao, K. H. Mess, M. Tigner, and F. Zimmermann (eds.), *Handbook of Accelerator Physics and Engineering*, Singapore: World Scientific, 2013.
- [15] Y. Shobuda *et al.*, “Reducing the beam impedance of the kicker at the 3-GeV rapid cycling synchrotron of the Japan Proton Accelerator Research Complex”, *Phys. Rev. Accel. Beams*, vol. 21, 061003, Jun. 2018; <https://journals.aps.org/prab/abstract/10.1103/PhysRevAccelBeams.21.061003>
- [16] O. Takeda, Private communications.
- [17] J. Kamiya and K. Yamamoto, “Operation Status of J-PARC Rapid Cycling Synchrotron”, presented at the 10th Int. Particle Accelerator Conf. (IPAC’19), Melbourne, Australia, May 2019, paper TUPTS036, this conference.